

Emerging giant resonant exciton induced by Ta-substitution in anatase TiO₂: a tunable correlation effect

Z. Yong,^{1,2,3,4} P. E. Trevisanutto,^{2,5,3} L. Chiodo,^{6,7} I. Santoso,^{1,2} A. R. Barman,^{2,3}
T. C. Asmara,^{1,2,3} S. Dhar,^{1,4,8} A. Kotlov,⁹ A. Terentjevs,¹⁰ F. Della Sala,^{10,11}
V. Olevano,¹² M. Rübhausen,^{13,14} T. Venkatesan,^{1,3,4,*} and A. Rusydi^{1,2,3,†}

¹NUSNNI-NanoCore, National University of Singapore, Singapore 117576

²Singapore Synchrotron Light Source, National University of Singapore, 5 Research Link, Singapore 117603, Singapore

³Department of Physics, National University of Singapore, Singapore 117542

⁴Department of Electrical and Computer Engineering,
National University of Singapore, Singapore 117576

⁵Centre for Advanced 2D Materials and Graphene Research Centre,
National University of Singapore, Singapore, 117546

⁶Unit of Nonlinear Physics and Mathematical Modeling, Department of Engineering,
Università Campus Bio-Medico di Roma, Via Álvaro del Portillo 21, 00128, Rome, Italy

⁷Center for Life Nano Science @Sapienza, Istituto Italiano di Tecnologia, Viale Regina Elena 291, 00161, Rome, Italy

⁸Department of physics, School of Natural Sciences, Shiv Nadar University,
Gautam Buddha Nagar, P.O. NH-91, Uttar Pradesh 201314, India

⁹Photon Science at DESY, Notkestraße 85. D-22607 Hamburg, Germany

¹⁰Istituto di Nanoscienze-CNR, Euromediterranean Center for Nanomaterial
Modelling and Technology (ECMT), Via per Arnesano 73100 Lecce, Italy

¹¹Center for Biomolecular Nanotechnologies @UNILE,
Istituto Italiano di Tecnologia, Via Barsanti, I-73010 Arnesano, Italy

¹²CNRS, Institut Néel, Grenoble, France

¹³Institute of Nanostructure and Solid State Physics,
Jungiusstrasse 11, 20355, University of Hamburg (Germany).

¹⁴Center for Free-Electron Laser Science, Advanced Study Group of the University of Hamburg,
Luruper Chaussee 149, 22761 Hamburg (Germany)

(Dated: September 15, 2021)

Titanium dioxide (TiO₂) has rich physical properties with potential implications in both fundamental physics and new applications. Up-to-date, the main focus of applied research is to tune its optical properties, which is usually done via doping and/or nano-engineering. However, understanding the role of *d*-electrons in materials and possible functionalization of *d*-electron properties are still major challenges. Herewith, within a combination of an innovative experimental technique, high energy optical conductivity, and of the state-of-the-art *ab initio* electronic structure calculations, we report an emerging, novel resonant exciton in the deep ultraviolet region of the optical response. The resonant exciton evolves upon low concentration Ta-substitution in anatase TiO₂ films. It is surprisingly robust and related to strong electron-electron and electron-hole interactions. The *d*- and *f*- orbitals localization, due to Ta-substitution, plays an unexpected role, activating strong electronic correlations and dominating the optical response under photoexcitation. Our results shed light on a new optical phenomenon in anatase TiO₂ films and on the possibility of tuning electronic properties by Ta substitution.

I. INTRODUCTION

Doped or defective titanium dioxide (TiO₂) exhibits rich physical phenomena in electronic transports and optical properties¹⁻⁴. TiO₂ is opaque in the visible sun light whereas it is very efficient in absorbing ultraviolet (UV) light rendering it interesting especially for photocatalysis applications⁵. The first step of photoexcitation is the formation of electron-hole pair quasiparticles (excitons), which may either recombine or decay into free charges. Eventually the free charges react with molecules on the surface enhancing photocatalytic effects and formation of reactive free radicals⁶. Excitons, and their spatial behaviour, play therefore a key role for both fundamental physics as well as for applications, but the precise nature and behaviour of excitons in TiO₂ based materials

remains unclear in some respects.

The many-body electron-electron (e-e) and electron-hole (e-h) interactions determine the physical properties of excitons, with different contributions depending on the system and on the considered energy range. Excitons usually occur below direct bandgap in semiconductor and insulator materials, but they may involve higher energy bands in the case of strong electronic correlation. With the recent development of supercomputing and *ab initio* calculations⁷⁻⁹, theoretical studies have shown that when both e-e and e-h interactions are strongly coupled, they yield to a new type of optical phenomenon, the so-called high-energy resonant excitonic effect. In fact, resonant excitons have been predicted^{10,11} and later observed^{12,13} in two-dimensional graphene. Unlike excitons in conventional semiconductors, the resonant excitons can occur at

energies even well above the corresponding optical band gap of the material, and they can be probed directly using high-energy optical conductivity¹³. A detailed understanding of the role of e-e and e-h interactions in TiO₂ based materials remains elusive, and resonant excitons have not been observed in the material, mainly because both experimental and theoretical studies at high-energy optical conductivity are challenging and limited in number.

We report in this paper on optical studies of TiO₂ doped at different concentrations of Tantalum, via optical conductivity measurements and *ab initio* Time Dependent Density Functional Theory (TDDFT) calculations. We have observed resonant excitonic effects in the deep-ultraviolet (DUV) in anatase Ta_xTi_{1-x}O₂ films, with only a small amount of Ta-substitution. A series of unusual phenomena arise, in particular the spectral-weight transfer from high towards low energies, and the emergence of an intense resonant exciton at ~ 6 eV. Based on our theoretical calculations, we relate these effects to a peculiar manifestation of strong e-e and e-h interactions. The paper is organized as follows: in section II, experimental and theoretical-computational used techniques are described. In section III, optical spectra, both measured and calculated, are described. In section IV, the main conclusions are drawn.

II. MATERIALS AND METHODS

Details of samples preparation and characterization, optical conductivity measurements and theoretical calculations are described in this section.

A. Experimental techniques

The optical conductivity was obtained using a combination of spectroscopic ellipsometry (0.5 – 5.6 eV) and UV-VUV reflectivity (3.7 – 35 eV) measurements^{14,15}. The spectroscopic ellipsometry measurements were performed in the spectral range between 0.5 and 5.6 eV by using an SE 850 ellipsometer at room temperature. Three different incidence angles of 60°, 70° and 80° from the sample normal were used, and the incident light was 45° linearly polarized from the plane of incidence. For reflectivity measurements in the high-energy range between 3.7 and 35 eV, we used the SUPERLUMI beamline at the DORIS storage ring of HASYLAB (DESY). The incoming photon was incident at an angle of 17.5° from the sample normal with linear polarization parallel to the sample surface. The sample chamber was outfitted with a gold mesh to measure the incident photon flux after the slit of the monochromator. The measurements were performed in ultra-high vacuum environment (chamber pressure of 5×10^{-10} mbar) at room temperature. Before these measurements, the samples were heated up to 400 K in ultra-high vacuum to ensure that there were

no additional adsorbate layers on the surface of the samples. The obtained UV-VUV reflectivity data were calibrated by comparing it with the luminescence yield of sodium salicylate (NaC₇H₅O₃) and the gold mesh current. These as-measured UV-VUV reflectivity data were further normalized by using the self-normalized reflectivity extracted from spectroscopic ellipsometry¹⁶.

B. Experimental samples and preparations

Ta₂O₅ and TiO₂ powders with high-purity (99.999%) were ground for several hours before sintering in a furnace at 1000°C in air for 20 h. Subsequently, target pellets were made and sintered at 1100°C in air for 24 h. Anatase Ta_xTi_{1-x}O₂ epitaxial thin films (with x=0, 0.018 and 0.038) of thickness 280 nm were deposited on high-quality (001) LaAlO₃ substrates by Pulsed Laser Deposition, using a 248 nm Lambda Physik excimer laser with an energy density of 1.8 J cm⁻² and a repetition rate of 210 Hz. Depositions were performed for 0.51 h in a stable oxygen partial pressure of 1×10^{-5} Torr while the substrate temperature was maintained at 750 °C. The chemical and structural properties of the samples were studied by X-ray Photoelectron Spectroscopy, electrical transport measurements, Rutherford backscattering spectrometry (RBS)/channelling, X-ray diffraction (XRD) and time-of-flight secondary-ion mass spectrometry (TOF-SIMS) as reported elsewhere^{17,18}. Ion channelling measurements indicated near perfect substitutional Ta atoms in Ti sites.

C. Theoretical and computational methods

All ground state electronic calculations are carried out by using Density Functional Theory (DFT) based on Quantum Espresso²⁸ and Abinit²⁹ codes, with the Perdew-Burke-Ernzerhof (PBE)-GGA approximation for the exchange-correlation functional³⁰. Norm conserving pseudopotentials in Troullier-Martins scheme³¹ are used, and semicore electrons are included in Ti and Ta pseudopotentials. The cutoff energy for the expansion of plane-wave basis is up to 170 Ry²². For pristine anatase TiO₂, we used a 12×12×8 Monkhorst-Pack k-point mesh sampling the Brillouin zone. For anatase Ta-TiO₂ bulk we used supercells with 48 atoms and a 4×4×4 Monkhorst-Pack k-point mesh grid. One Ti atom is replaced with one Ta atom (substitutional doping, modelling a 6.5 % Ta-doping in TiO₂ bulk almost equivalent to the experimental doped sample (3.8 %)).

The excited state calculations have been performed within two approaches: solving the Bethe Salpeter Equation (BSE, which implicitly includes both e-h and e-e interactions), and applying the jellium with gap model (JGM) kernel²⁴ within the Time Dependent Density Functional Theory (TDDFT). The latter method includes the e-e and e-h interactions maintaining the com-

putational feasibility for such compelling calculations. The complex dielectric function has also been evaluated at the random phase approximation (RPA) level, with electrons and holes treated as independent particles, without correlation. The Bethe-Salpeter Equation has been solved using Yambo code³² and EXC³³. The screening dielectric matrix has been evaluated by using the static inverse dielectric function, with cutoffs of 21 Ry for the correlation (exchange) part, and unoccupied states are summed over 176 empty states. In BSE calculations defined hereafter as Low Resolution (LR), 28 occupied bands and 52 empty bands are included in the diagonalization, to describe the region above 5 eV, on a k-point grid of $4 \times 4 \times 2$. For the High Resolution (HR) BSE calculation, used to describe in more detail the adsorption threshold, 8 occupied and 8 empty bands are included in the diagonalization, on a $12 \times 12 \times 12$ k-point grid. Haydock recursive approach for diagonalization is used, with threshold accuracy of -0.02. The DP-EXC code³⁴ is used for the TDDFT calculations. In pristine TiO_2 bulk, 200 bands are included for the RPA and JGM-TDDFT calculations.

III. RESULTS AND DISCUSSION

Here, we provide some general information on pure TiO_2 , useful in the following discussion on optical conductivity. The electronic ground state structure of pristine and doped TiO_2 , based on DFT results for total Density of States (DOS) and Partial DOS (PDOS), is shown in Fig. 1. The DFT-PBE band gap of pristine TiO_2 is ~ 2.20 eV. The valence band (Fig. 1-(a)) mainly consists of O 2p orbitals slightly hybridized with Ti 3d orbitals. The conduction band is comprised by Ti 3d orbitals with a small hybridized amount O 2p orbitals.

In Ta- TiO_2 (Fig. 1-(b)), the 3d Ta orbitals fill the bottom of conduction band, making the system metallic, and they are hybridized with the adjacent O 2p orbitals up to 8 eV in the conduction band. The proper inclusion of correlation removes this spurious metallicity described by DFT, as shown for Nb-doped rutile³⁵. Main features of electronic band structure (Fig. 2-(a)) and optical absorption spectrum of anatase TiO_2 have been studied for a long time, and they have been deeply revised and reanalyzed recently³⁶.

Next, we focus on the large spectral changes induced by Ta-doping on the optical response, even for small amounts of Ta-substitution. Fig. 3 shows the optical conductivity of TiO_2 and Ta-doped TiO_2 films, at increasing Ta-doping and on a broad energy range, up to ~ 35 eV. $\text{Ta}_x \text{Ti}_{1-x} \text{O}_2$ films are measured for $x = 0, 0.018$ and 0.038 . For $x = 0$, the pure TiO_2 sample, we observe a first sharp optical excitation at 3.48 eV (P1, see inset Fig. 3), followed by bulk resonances from 3.85 eV to 4.6 eV (P2)³⁶. A well-defined large peak, at ~ 6.12 eV (P3), is a newly observed intense bulk resonance in pure TiO_2 . It is followed by broad and multiple structures up

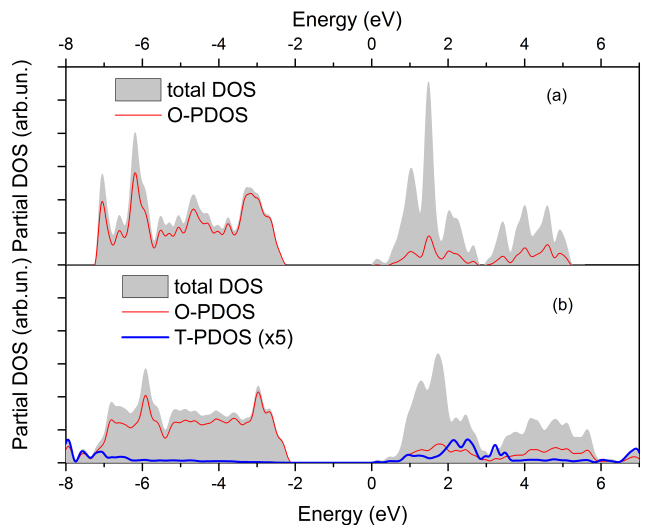


FIG. 1. (a) Total DOS of anatase TiO_2 from DFT calculations. Black line is referred to the total DOS. Red line is the Oxygen partial DOS. (b) DOS of 6.5 % Ta-substituted anatase TiO_2 . The blue line is the partial DOS of Ta atom multiplied by a factor 5 to make more clear the peaks position.

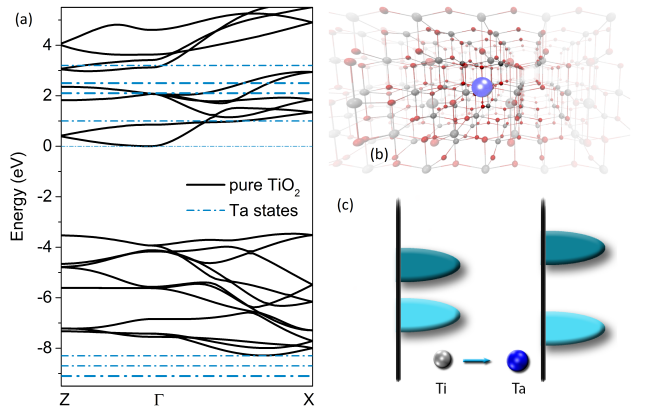


FIG. 2. (a) Anatase band structure (black line), along the high-symmetry directions Z- Γ -X of Brillouin Zone. A scissor of 1.2 eV has been applied on top of PBE-DFT band structure. Ta-derived states, extrapolated from the PDOS analysis, has been superimposed on the pristine TiO_2 band structure (blue dashed line). We can rule out a direct effect of Ta-doping on optical properties, as optical transitions involving Ta-states neither coincide in energy with peaks observed in optical conductivity, neither the PDOS associated to the low Ta-doping here considered could generate the intense optical features we observed. (b) A graphical representation of the long-range correlation effects of the low Ta-doping in TiO_2 anatase crystal. (c) A simplified cartoon representation of the effects of Ti - Ta substitution that turns on the on-site Coulomb repulsion involving d-Ti and p-O states. The on-site repulsive interaction induces a bandgap opening, giving optical transitions above the optical gap.

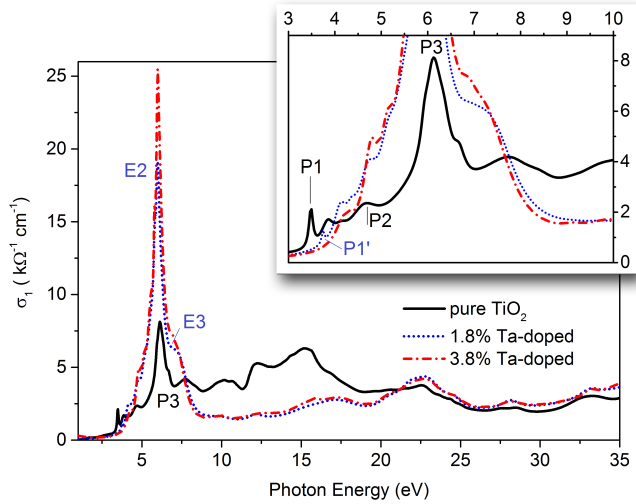


FIG. 3. Room temperature measurements of the real part of the optical conductivity for pure TiO_2 (solid black line), 1.8% (blue short dotted line), and 3.8% Ta-substituted TiO_2 (red dashed-dotted line). The polarization vector is perpendicular to the $[001]$ direction. Inset: details of the real part of the optical conductivity in the VIS and low UV regions.

to ~ 35 eV.

Upon Ta-substitution ($x=0.018$) we observe an emerging new giant peak at 6.0 eV (E2, Fig. 3), three times more intense than the P3 peak of pure anatase. At 6.8 eV there is an intense shoulder (E3) of the giant peak E2. The first optical excitation is also affected by Ta-doping, as it occurs at higher energy (3.75 eV, P1') and reduced in intensity with respect to the pure sample. Furthermore, upon substitutional doping, the spectrum shows a significant reduction of the spectral-weight in a broad energy range (from ~ 8 eV to ~ 20 eV) and a slight spectral-weight gain, singular at even higher energy (from ~ 20 eV to ~ 35.0 eV). For higher Ta-concentration ($x=0.038$), the E2 at 6.0 eV peak shows further enhanced intensity, without any significant change in the remaining structures with respect to lower Ta-concentration. To summarize, we have, upon Ta-doping: (i) an anomalous spectral-weight transfer from energies as high as 35 eV towards the 6 eV region; (ii) the emergence of a novel resonant exciton E2 at 6 eV; and (iii) the strong modification of TiO_2 optical conductivity, with an augmented optical bandgap. The optical conductivity here measured in such a broad energy range results crucial to investigate the nature of E2. Based on the optical f -sum rule, we find that the total spectral-weight (up to 35 eV) is nearly conserved for all three investigated doping ratios (Fig. 3). This directly implies that the oscillator strength at 6.0 eV is coming from spectral-weight transfers of the higher bands, i.e. from 8 to 20 eV. Such a collective spectral-weight transfer is a fingerprint of strong electronic correlations¹⁹⁻²¹. Our theoretical analysis (see below) shows that the E3 peak in $\text{Ta}_x\text{Ti}_{1-x}\text{O}_2$ has similar origin as the P3 peak at 6.12 eV in undoped TiO_2 ,

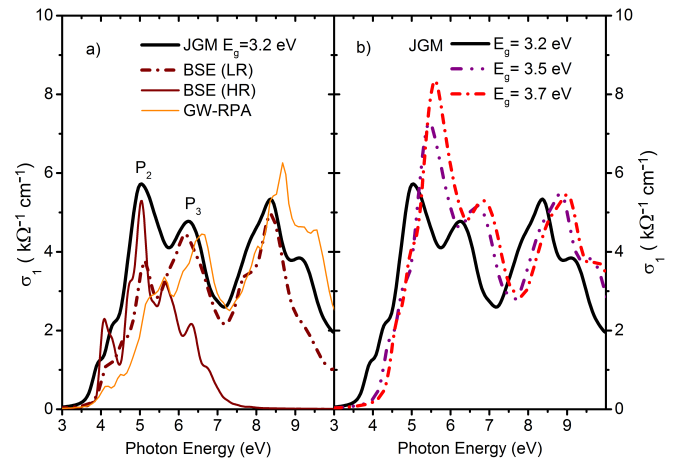


FIG. 4. (a) The calculated optical conductivity ($[001]$ in-plane polarization) for anatase TiO_2 in the GW-RPA approximation (orange solid line), solving the Bethe-Salpeter equation in low resolution (LR-BSE, dark red dashed-dotted line) and High Resolution BSE (HR-BSE, dark red solid line), and within TDDFT using the JGM kernel with $E_g = 3.2$ eV - experimental indirect bandgap of TiO_2 (black solid line). The HR-BSE calculations include more stringent convergence parameters but with less included conduction bands. The LR-BSE calculations are performed to describe high energy features (beyond 6 eV). Both of them are performed to validate the JGM-TDDFT calculations. (b) Optical conductivity ($[001]$ in-plane polarization) for anatase $\text{Ta}_x\text{Ti}_{1-x}\text{O}_2$ calculated by TD-DFT with JGM kernel and E_g of 3.2 eV (solid black line), 3.5 eV (dotted purple line), and 3.7 eV (dashed-dotted red line). Increasing E_g results in an enhanced peak at 6 eV.

while E2 can be associated to an evolution of the bulk resonance P2. Further, based on our theoretical calculations, we could investigate the role of e-e and e-h interactions, clarifying the nature of the giant exciton E2 and confirming that observed optical behaviour is due to a manifestation of strong e-e and e-h interactions.

In Fig. 4 (a), we show the optical conductivity of the pure TiO_2 calculated using the three above mentioned theoretical methods. The GW-BSE calculations, taking into account both the e-e and e-h interactions, give rise to bound and resonant excitons or other excitonic effects along with spectral-weight transfers. The comparison between the GW-BSE and GW-RPA results gives therefore a direct measure of the excitonic nature of a resonance. The GW-RPA calculation fails in reproducing the P2 bulk resonance and the structures near the absorption edges, while both GW-BSE and JGM-TDDFT, with some differences in their detail, are able to describe the P1 and P2 peaks. This confirms that the e-e and e-h interactions are significant and important, not only for doped anatase, but even for pure TiO_2 , in agreement with previous results^{22,23}. We plot here the optical conductivity, but we note that our GW-BSE result (HR) for optical absorption (not shown) is comparable with previous calculations for TiO_2 dielectric function^{12,13,19,36}.

From Ref.^{22,36}, we know that the P1 peak (experimentally at ~ 3.48 eV) related to bound exciton whereas P2 (at ~ 4.6 eV) comes from a bulk resonance.

The LR and HR GW-BSE data allow to properly align and identify the JGM-TDDFT spectral features with respect to experimental data, having as reference the P2 peak. The JGM-TDDFT and HR-GW-BSE coincide in intensity and energy for the peak P2, whereas, for the peak P3 and higher energy features, LR-GW-BSE calculations are in good agreement with the JGM-TDDFT. Upon Ta-substitution, the solution of the GW-BSE becomes computationally cumbersome. We turn therefore to JGM-TDDFT, which is equally reliable, as just shown in the case of pure TiO_2 , but computationally feasible also for large supercells.

We focus on optical features in the region of the ~ 6.0 eV, and we use TDDFT to qualitatively study the relationship between E_g (and therefore the screening properties of the material), and resonant excitonic effects in $\text{Ta}_x\text{Ti}_{1-x}\text{O}_2$. In Fig. 4(b), we show JGM-TDDFT results for increasing band-gap values, $E_g = 3.2, 3.5, 3.7$ eV for $\text{Ta}_x\text{Ti}_{1-x}\text{O}_2$. The strong correlation mimicked by E_g is reflected in the optical response, in particular in the behaviour of the peak at 6.0 eV. Peak P2 undergoes a redshift of almost 1 eV, and at the same time its intensity increases. Other features in the spectrum (as P3) undergo a similar shift, but no intensity changes are observed other than for P2.

In Fig. 5-(a), we compare the experimental findings with the theoretical calculations. Even though the results differ in intensity, both P2 and P3 are present. Nevertheless, when the JGM-TDDFT with $E_g = 3.7$ eV is compared with the Ta- TiO_2 optical conductivity (Fig. 5-b), the theoretical calculations qualitatively suggest that peak P2 is evolving in the E2 exciton at 6.0 eV whereas the P3 peak at ~ 6.1 eV is transforming in the shoulder E3 at 6.8 eV (Fig 5(b)). This seems to be counter-intuitive looking at only the experimental optical conductivity results for pure and Ta-substituted TiO_2 , but becomes clear when the proper alignment and assignment of optical features are performed. From the current results, it seems that E2, evolving from P2, is indeed a resonant exciton emerging from an electron-hole continuum which exists at higher energy bands, well beyond a continuum spectrum.

Our JGM-TDDFT calculations display an interplay between E_g and the resonant excitons, i.e. larger E_g reflects in an enhancement of the resonant excitonic effects. Furthermore, the JGM-TDDFT calculations support the following scenario: the resonant exciton E2 at ~ 6 eV in experimental spectra can be related to a modification of the electronic structure under Ta-substitution, leading also to the opening of the bandgap. This result is in contrast to a conventional picture, where Ta-substitution would lead to a simple electron doping and metallization of TiO_2 . In fact, our findings imply that Ta-substitution in $\text{Ta}_x\text{Ti}_{1-x}\text{O}_2$ does not act as a conventional dopant, but plays instead an unusual role in enhancing strong

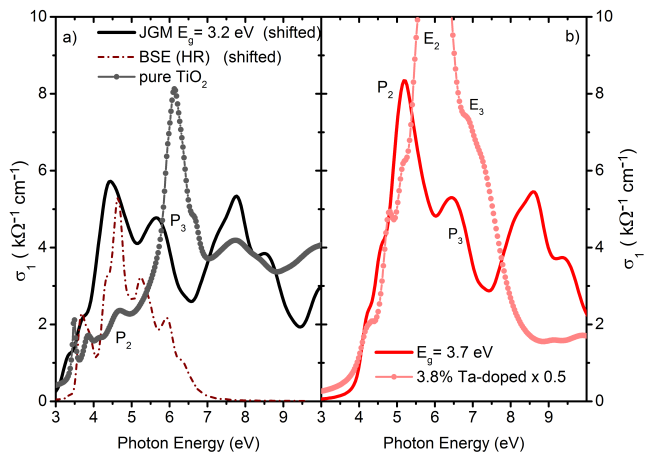


FIG. 5. (a) Comparison between experimental (grey ball lines) and BSE (dot-dashed dark red) and JGM-TDDFT ($E_g = 3.2$ eV, black solid line) Optical conductivity calculations for pure anatase TiO_2 . A rigid shift of -0.6 eV has been applied to align the theoretical spectra to experimental data. (b) Experimental optical conductivity (pink balls) and JGM-TDDFT calculations (solid red line) for Ta-substituted (3.8% TiO_2 with $E_g = 3.7$ eV). A rigid shift of -0.6 eV has been applied to align the theoretical spectra to experimental data.

electronic correlations. A behavior partaking some similarities with these results has been recently reported for a magnetic-doped TiO_2 system. Theoretical investigation of magnetic Cr-doped TiO_2 ²⁵ shows that upon Cr-doping the electronic properties undergo a transformation, and the (initially Charge Transfer insulator) system becomes a strongly correlated Mott-Hubbard crystal. We observe here an optical response which is consequent to an analogous effect in the electronic structure: the excitonic strength resulting in an enhancement of the absorption peak is occurred by the band gap opening. Upon electron doping via Ta-substitution, a possible scenario about the increasing electronic correlation is related to the Ti d-d and Ti d - O p orbital repulsions, but a more detailed analysis is left to frameworks with a better treatment of strongly correlated interactions. The scenario for Ta-doped TiO_2 optics presents conceptual similarities to strong correlated materials, as cuprates like doped $\text{La}_{2-x}\text{Sr}_x\text{CuO}_4$ ^{26,27}. In this respect, TiO_2 is widely considered an intermediate oxide between the Charge Transfer insulator and Mott-Hubbard regimes^{37,38}. We observe some analogies between our Ta-doped semiconductor spectra, and the optical behaviour of undoped Mott insulators (as cuprates), where intense optical absorption in the DUV are due to transitions from the lower to the upper Hubbard band. In the case of Mott-insulators, the change of E_g (or the Mott-gap²³) as function of doping gives a signature of the e-e correlation. By using the Dynamical Mean Field Theory (DMFT), it has been shown that different percentages of doping enable a change of phase. The increase of d-states modifies their electronic Density Of States (DOS), and the pseudo-gap material

becomes insulating. This results in a strong enhancement of peaks intensity in the optical conductivity. A similar behavior may be revealed in the present case where the inclusion of Ta d- and f- orbitals seems to have a role in changing the TiO₂ physics increasing both e-e and e-h correlations.

IV. CONCLUSIONS

In conclusion, we have presented the emergence of an intense resonant exciton induced by Ta-substitution in anatase TiO₂. This result is of primary importance for possible industrial applications. We argue that in these experimental findings tunable e-e and e-h correlations play a key role in the observed resonant excitons in Ta_x Ti_{1-x}O₂ system, and can be used in a model for resonant excitonic effects. Further works will be devoted to improve our qualitative description in a more quantitative agreement with the experimental results.

It is then also important for future theoretical study

to explicitly include the on-site Coulomb repulsion in the optical spectra calculations.

V. ACKNOWLEDGMENTS

This work is supported by Singapore National Research Foundation under its Competitive Research Funding (NRF-CRP 8-2011-06), MOE-AcRF Tier-2 (MOE2015-T2-1-099), and FRC. We acknowledge the CSE-NUS computing centre, Centre for Advanced 2D Materials and Graphene Research Centre for providing facilities for our numerical calculations. We also acknowledge the National Research Foundation, Prime Ministers Office, Singapore, under its Medium Sized Centre Programme and Competitive Research Funding (R-144-000-295-281). L.C. acknowledges M. Lauricella and J. Sofo for useful discussions. Authors acknowledge F. Da Pieve for a critical reading of the manuscript. Z.Y., P.E.T. and L.C. contributed equally.

-
- * venky@nus.edu.sg
 † phyandri@nus.edu.sg
- ¹ O. Dulub et al., *Electron-Induced Oxygen Desorption from the TiO₂(011)-21 Surface Leads to Self-Organized Vacancies*. Science 317, 1052-1056 (2007).
 - ² E. J. W. Crossland et al., *Mesoporous TiO₂ single crystals delivering enhanced mobility and optoelectronic device performance*. Nature 495, 215-219 (2013).
 - ³ C. Richter, C. A. Schmuttenmaer, *Exciton-like trap states limit electron mobility in TiO₂ nanotubes*. Nature nanotechnology 5, 769-772 (2010).
 - ⁴ B. O'regan, M. Grätzel, *A low-cost, high-efficiency solar cell based on dye-sensitized colloidal TiO₂ films*. (1991).
 - ⁵ I. Chung, B. Lee, J. He, R. P. H. Chang, M. G. Kanatzidis, *All-solid-state dye-sensitized solar cells with high efficiency*. Nature 485, 486-489 (2012).
 - ⁶ E. W. McFarland, J. Tang, *A photovoltaic device structure based on internal electron emission*. Nature 421, 616-618 (2003).
 - ⁷ S. Albrecht, L. Reining, R. Del Sole, G. Onida, *Ab Initio Calculation of Excitonic Effects in the Optical Spectra of Semiconductors*. Phys. Rev. Let. 80, 4510-4513 (1998).
 - ⁸ L. X. Benedict, E. L. Shirley, R. B. Bohn, *Optical Absorption of Insulators and the Electron-Hole Interaction: An Ab Initio Calculation*. Phys. Rev. Let. 80, 4514-4517 (1998).
 - ⁹ M. Rohlfing, S. G. Louie, *Electron-Hole Excitations in Semiconductors and Insulators*. Phys. Rev. Let. 81, 2312-2315 (1998).
 - ¹⁰ L. Yang, J. Deslippe, C.-H. Park, M. L. Cohen, S. G. Louie, *Excitonic Effects on the Optical Response of Graphene and Bilayer Graphene*. Phys. Rev. Let. 103, 186802 (2009).
 - ¹¹ P. E. Trevisanutto, M. Holzmann, M. Ct, V. Olevano, *Ab initio high-energy excitonic effects in graphite and graphene*. Phys. Rev. B 81, 121405 (2010).
 - ¹² K. F. Mak, J. Shan, T. F. Heinz, *Seeing Many-Body Effects in Single- and Few-Layer Graphene: Observation of Two-Dimensional Saddle-Point Excitons*. Phys. Rev. Let. 106, 046401 (2011).
 - ¹³ I. Santoso et al., *Observation of room-temperature high-energy resonant excitonic effects in graphene*. Phys. Rev. B 84, 081403 (2011).
 - ¹⁴ A. Rusydi et al., Physical Review B 78, 125110 (2008).
 - ¹⁵ T. C. Asmara et al., Nat. Comm. 5 (2014).
 - ¹⁶ T. C. Asmara, I. Santoso, and A. Rusydi, Review of Scientific Instruments 85, 123116 (2014)
 - ¹⁷ A. Rusydi et al., Philosophical Transactions of the Royal Society of London A: Mathematical, Physical and Engineering Sciences 370, 4927 (2012).
 - ¹⁸ D.-C. Qi et al., Physical Review B 87, 245201 (2013).
 - ¹⁹ H. Eskes, M. B. J. Meinders, G. A. Sawatzky, *Anomalous transfer of spectral weight in doped strongly correlated systems*. Phys. Rev. Let. 67, 1035-1038 (1991).
 - ²⁰ Y. Ohta, K. Tsutsui, W. Koshibae, T. Shimozato, S. Maekawa, *Evolution of the in-gap state in high-Tc cuprates*. Phys. Rev. B 46, 14022-14033 (1992).
 - ²¹ P. Phillips, *Colloquium : Identifying the propagating charge modes in doped Mott insulators*. Rev. of Modern Phys. 82, 1719-1742 (2010).
 - ²² L. Chiodo et al., *Self-energy and excitonic effects in the electronic and optical properties of TiO₂ crystalline phases*. Phys. Rev. B 82, (2010).
 - ²³ W. Kang, M. S. Hybertsen, *Quasiparticle and optical properties of rutile and anatase TiO₂*. Phys. Rev. B 82, (2010).
 - ²⁴ P. E. Trevisanutto, A. Terentjevs, L. A. Constantin, V. Olevano, F. D. Sala, *Optical spectra of solids obtained by time-dependent density functional theory with the jellium-with-gap-model exchange-correlation kernel*. Phys. Rev. B 87, (2013).
 - ²⁵ F. Da Pieve et al., *Origin of Magnetism and Quasiparticles Properties in Cr-Doped TiO₂*. Phys. Rev. Let. 110, 136402

- (2013).
- ²⁶ T. Das, R. S. Markiewicz, A. Bansil, *Strong correlation effects and optical conductivity in electron-doped cuprates*. Eur. phys. lett. **96**, 27004 (2011).
- ²⁷ C. Weber, K. Haule, G. Kotliar, *Optical weights and waterfalls in doped charge-transfer insulators: A local density approximation and dynamical mean-field theory study of $La_{2-x}Sr_xCuO_4$* . Phys. Rev. B **78**, 134519 (2008).
- ²⁸ P. Giannozzi et al., *QUANTUM ESPRESSO: a modular and open-source software project for quantum simulations of materials* Journal of Physics: Condensed Matter **21** 395502 (2009)
- ²⁹ X. Gonze et al., *ABINIT: First-principles approach to material and nanosystem properties* Comput. Phys. Comm. **180**, 2582 (2009).
- ³⁰ J. P. Perdew, K. Burke, and M. Ernzerhof, Phys. Rev. Lett. **77**, 3865 (1996)
- ³¹ N. Troullier, J. L. Martins. Efficient Pseudopotentials for Plane-Wave Calculations .2. Operators for Fast Iterative Diagonalization. Physical Review B **43**, 8861 (1991)
- ³² A. Marini, C. Hogan, M. Grüning and, D. Varsano. Yambo: An ab initio tool for excited state calculations. Comput Phys Commun **2009**, 180(8): 1392-1403.
- ³³ <http://www.bethe-salpeter.org>
- ³⁴ <http://www.dp-code.org>
- ³⁵ M. Zhang et al., *All-electron GW calculation of rutile TiO_2 with and without Nb impurities*, Phys. Rev. B **92**,035205
- ³⁶ E. Baldini, L. Chiodo, A. Dominguez, M. Palumbo, S. Moser, M. Yazdi, G. Aubeck, B. P. P. Mallett, H. Berger, A. Magrez, C. Bernhard, M. Grioni, A. Rubio, and M. Chergui, arXiv:1601.01244 [cond-mat] (2016), arXiv: 1601.01244.
- ³⁷ J. Zaanen, G.A. Sawatzky and, J.W. Allen, *Band gaps and electronic structure of transition-metal compounds*, Phys. Rev. Lett. **55** 418 (1985)
- ³⁸ A.E. Bocquet et al., *Electronic structure of early 3d-transition-metal oxides by analysis of the 2p core-level photoemission spectra*, Phys. Rev. B **53** 1161 (1996)